



Full Length Article

Impact of structure and morphology of nanostructured ceria coating on AISI 304 oxidation kinetics



R. Aadhavan, K. Suresh Babu*

Centre for Nanoscience and Technology, Madanjeet School of Green Energy Technologies, Pondicherry University (A Central University), Puducherry 605 014, India

ARTICLE INFO

Article history:

Received 23 November 2016

Received in revised form 21 February 2017

Accepted 13 March 2017

Available online 16 March 2017

Keywords:

PVD

Coating

Ceria

Nano

Surface

Oxidation

ABSTRACT

Nanostructured ceria-based coatings are shown to be protective against high-temperature oxidation of AISI 304 due to the dynamics of oxidation state and associated defects. However, the processing parameters of deposition have a strong influence in determining the structural and morphological aspects of ceria. The present work focuses on the effect of variation in substrate temperature (50–300 °C) and deposition rate (0.1–50 Å/s) of ceria in electron beam physical vapour evaporation method and correlates the changes in structure and morphology to high-temperature oxidation protection. Unlike deposition rate, substrate temperature exhibited a profound influence on crystallite size (7–18 nm) and oxygen vacancy concentration. Upon isothermal oxidation at 1243 K for 24 h, bare AISI 304 exhibited a linear mass gain with a rate constant of $3.0 \pm 0.03 \times 10^{-3} \text{ kg}^2 \text{ m}^{-4} \text{ s}^{-1}$ while ceria coating lowered the kinetics by 3–4 orders. Though the thickness of the coating was kept constant at 2 μm, higher deposition rate offered one order lower protection due to the porous nature of the coating. Variation in the substrate temperature modulated the porosity as well as oxygen vacancy concentration and displayed the best protection for coatings deposited at moderate substrate temperature. The present work demonstrates the significance of selecting appropriate processing parameters to obtain the required morphology for efficient high-temperature oxidation protection.

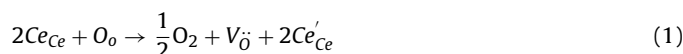
© 2017 Elsevier B.V. All rights reserved.

1. Introduction

Structural materials such as stainless steels possess good mechanical as well as corrosion resistance properties [1]. Austenitic stainless steel, having good formability and weldability, exhibits a variety of high-temperature applications such as in vanes, turbine blades, superheaters and fuel-conversion devices, etc [2,3]. Due to higher chromium content, a protective chromia (Cr_2O_3) layer forms over the stainless steel surface, which acts as a barrier layer against further oxidation [4,5]. However, prolonged exposure to high temperature accelerates the diffusion of other metallic elements through the passivating chromia scale to form a fragile spinel type AB_2O_4 (A, B are transition metals) layer thereby limiting the structural integrity [6]. The presence of rare earth elements such as Ce, La, Zr and Y in alloy matrix or surface coating have shown to improve the oxidation protection at high temperatures. The effect introduced by the incorporation of these elements to reduce the oxidation rate and increase the adhesion between the oxide layer

and the substrate is known as reactive element effect (REE) [5]. Various methodologies have been reported to bring about surface modification without altering the properties of the substrate.

Nanostructured cerium oxide (ceria, CeO_2) has a unique redox property which arises from the existence of cerium in dual oxidation states of +3 and +4. In response to size, the presence of dopant as well as the environmental factors, the oxidation state of cerium changes due to the lower interconversion energy between the two oxidation states [7–9]. Conversion of two Ce^{4+} to two Ce^{3+} generates an oxygen vacancy defect in the lattice, to maintain the charge neutrality in the ceria lattice, as represented by Kröger–Vink notation



where Ce_{Ce} denotes Ce^{4+} in cerium lattice, O_{O} represents oxygen in oxygen lattice, V_{O} indicates oxygen vacancy and Ce'_{Ce} signifies Ce^{3+} in cerium lattice. Stability of cubic fluorite structure till the melting point and the formation of defects that enable the storage of oxygen, redeem ceria as a valuable material for the applications such as electrolyte in solid oxide fuel cells, the three-way catalyst in automobile exhausts, gas sensors, etc [10–13].

* Corresponding author.

E-mail address: sureshbabu.nst@pondiuni.edu.in (S.B. K.).

Table 1Sample detail, crystallite size, defect concentration (N) and rate constant (k_p) for nanoceria coated samples before and after oxidation for various deposition rates.

| Sample code | Deposition rate (Å/s) | Substrate Temperature (°C) | Crystallite size, nm | | Defect concentration, $N \times 10^{21} \text{ (cm}^{-3}\text{)}$ | | Defect ratio ^a | Rate constant, k_p ($\text{kg}^2 \text{ m}^{-4} \text{ s}^{-1}$) |
|-------------|-----------------------|----------------------------|----------------------|-----------------|---|-----------------|---------------------------|--|
| | | | Before oxidation | After oxidation | Before oxidation | After oxidation | | |
| AISI304 | – | – | – | – | – | – | – | $3.0 \pm 0.03 \times 10^{-3}$ |
| 0.1 Å/s | 0.1 | 100 | 7.4 | 35.4 | 2.01 | 0.715 | 2.81 | $3.1 \pm 0.01 \times 10^{-7}$ |
| 1 Å/s | 1 | 100 | 7.8 | 36.3 | 2.04 | 0.725 | 2.81 | $5.4 \pm 0.02 \times 10^{-7}$ |
| 10 Å/s | 10 | 100 | 8.5 | 38.3 | 2.01 | 0.734 | 2.74 | $2.9 \pm 0.04 \times 10^{-6}$ |
| 25 Å/s | 25 | 100 | 8.6 | 39.7 | 2.03 | 0.745 | 2.72 | $5.8 \pm 0.02 \times 10^{-6}$ |
| 50 Å/s | 50 | 100 | 9.1 | 39.9 | 2.02 | 0.750 | 2.70 | $7.4 \pm 0.01 \times 10^{-6}$ |

^a The ratio of oxygen vacancy concentration for the coatings before and after oxidation.

Various researches have investigated the effect of tuning the physical properties of superficially coated ceria towards the protection of the stainless steels from high-temperature oxidation. It has been shown that microceria coatings significantly improve the protection of stainless steels such as AISI 304, 316 and 321 against oxidation at 1423 K by suppressing the outward migration of cations [14]. Fe-Cr alloys coated with a slurry containing CeO_2 powder dispersed in ethanol rendered better protection than the uncoated alloys at 923 K [15]. The effect of microceria and nanoceria coated by sol-gel/microemulsion method technique on the oxidation protection of AISI 304 at 1260 K is compared and reported that the efficiency of ceria nanoparticles in preventing oxidation [13]. The role of Ce^{3+} or oxygen vacancy concentration in nanostructured ceria was envisaged to provide the additional effect on improving high-temperature oxidation protection [16]. Viswanathan et al. was reported that the solution precursor plasma spray (SPPS) coated nanoceria rendering two orders of better protection against oxidation in comparison to uncoated sample [17]. Lopez et al. reported that dip coating does not give uniform coverage for nanoceria coating which results in the formation of Fe-rich islands during oxidation at 1273 K [18].

From the literature, it can be seen that not only the coating material but the nature of the coating such as thickness, surface morphology is also important for designing the materials for high-temperature protection. The reported techniques like sol-gel, spray and dip coating results in non-uniform and porous coatings and thereby, influencing the oxidation protection [9,13,17,18]. In an earlier study, we have reported the use electron beam physical vapour deposition (EBPVD) in precisely controlling the thickness of ceria nanostructure in order to arrive at the threshold thickness for efficient protection at high temperatures [19]. The thickness of the coating influences the oxygen partial pressure at the substrate/nanoceria interface, thereby varying the tendency towards oxidation. Though the role of ceria thickness on oxidation has been investigated, it is important to optimize the process parameters such as deposition rate and substrate temperature at a fixed thickness to correlate with the surface morphological features. In the present work, we report the effect of deposition rate and the substrate temperature on structure/morphology while maintain-

ing the ceria thickness at 2 μm and its effect on higher temperature oxidation protection.

2. Experimental

Nanocrystalline ceria powder was synthesized by chemical precipitation method as reported earlier [19]. Briefly, to 0.06 M cerium nitrate hexahydrate (Himedia, $\geq 99.99\%$), 1N ammonium hydroxide (Himedia, Analytical Grade) was added dropwise while maintaining the pH at 10. The resultant precipitate was washed three times with deionized water and dried at 353 K for 8 h. Cylindrical pellets made by pressing the powder at 5 ton were sintered at 1473 K for 5 h to form the target required for electron beam deposition. The chemical composition (in weight percentage) of the AISI 304 stainless steel substrate used in the present study is C, 0.08; Cr, 18.35; Mn, 1.84; Ni, 8.54; P, 0.045; S, 0.030; Si, 1.00; the balance being Fe. AISI 304 coupons of $15 \times 15 \text{ mm}$ dimension were cut from 3 mm thick stainless steel plate. The substrate surface was polished using 1200 grit SiC paper and subsequently cleaned with isopropanol in an ultrasonicator.

The deposition was carried out using EBPVD (Hind High Vacuum, Bangalore, Model: BC-300 vacuum box coater) with a base pressure of $3.75 \times 10^{-6} \text{ Torr}$. Two processing parameters, deposition rate, and substrate temperature were investigated, to cognize the role of each on the structure and morphology. First, the deposition rate was varied from 0.1, 1, 10, 25 and 50 Å/s, while maintaining the substrate temperature at 100 °C. The deposition rate was varied by tuning the filament current while keeping the voltage constant at 5 keV for all the samples. In the second part of the study, the deposition was carried out at different substrate temperatures of 50, 100, 200 and 300 °C sample coded as 50ST, 100ST, 200ST, and 300ST, respectively, at a fixed deposition rate of 0.1 Å/s. The thickness of the film during the deposition was monitored using *in situ* digital thickness monitor and subsequently confirmed by a profilometer (Dektak 6, Veeco, USA). A coating thickness of 2 μm was maintained and the sample details are given in Tables 1 and 2.

A custom-made computer controlled set-up was used to monitor the mass change in real time to evaluate the high-temperature oxidation protection. Isothermal oxidation tests were carried out

Table 2Sample details, mean crystallite size, defect concentration (N) and rate constant (k_p) for nanoceria coated samples before and after oxidation at different substrate temperatures.

| Sample code | Deposition rate (in Å/s) | Substrate Temperature (in °C) | Crystallite size (nm) | | Defect concentration, $N \times 10^{21} \text{ (cm}^{-3}\text{)}$ | | Defect ratio ^a | Rate constant k_p , ($\text{kg}^2 \text{ m}^{-4} \text{ s}^{-1}$) |
|-------------|--------------------------|-------------------------------|-----------------------|-----------------|---|-----------------|---------------------------|---|
| | | | Before oxidation | After oxidation | Before oxidation | After oxidation | | |
| AISI304 | – | – | – | – | – | – | – | $3.0 \pm 0.03 \times 10^{-3}$ |
| 50ST | 0.1 | 50 | 7.8 | 34.8 | 2.42 | 0.844 | 2.87 | $7.2 \pm 0.03 \times 10^{-6}$ |
| 100ST | 0.1 | 100 | 8.0 | 36.7 | 2.05 | 0.791 | 2.58 | $3.5 \pm 0.02 \times 10^{-7}$ |
| 200ST | 0.1 | 200 | 15.4 | 39.7 | 1.50 | 0.772 | 1.94 | $3.4 \pm 0.03 \times 10^{-6}$ |
| 300ST | 0.1 | 300 | 17.5 | 40.6 | 1.33 | 0.763 | 1.74 | $5.4 \pm 0.05 \times 10^{-6}$ |

^a The ratio between oxygen vacancy concentration between before and after oxidation.

Download English Version:

<https://daneshyari.com/en/article/5347111>

Download Persian Version:

<https://daneshyari.com/article/5347111>

[Daneshyari.com](https://daneshyari.com)